

Article

Effect of Ion-Exchange Sequences on Catalytic Performance of Cerium-Modified Cu-SSZ-13 Catalysts for NH₃-SCR

Yan Wang^{1,2}, Zhaoqiang Li^{1,2,*} , Zhiyong Ding^{1,2}, Na Kang^{1,2}, Rongrong Fan^{1,2}, Yu Wang^{1,2}, Cheng Zhang^{1,2}, Xin Guo^{1,2} and Rong Wang^{1,2}

¹ State Key Laboratory of Baiyunobo Rare Earth Resource Researches and Comprehensive Utilization, Baotou Research Institute of Rare Earths, Baotou 014030, China; wangyan@brire.com (Y.W.); dingzhiyong@brire.com (Z.D.); kangna@brire.com (N.K.); fanrongrong@brire.com (R.F.); wangyu2021@brire.com (Y.W.); zhangcheng2021@brire.com (C.Z.); guoxin@brire.com (X.G.); wangrong@brire.com (R.W.)

² National Engineering Research Center of Rare Earth Metallurgy and Functional Materials, Baotou 014030, China

* Correspondence: lizq@brire.com; Tel.: +86-151-4939-4414

Abstract: Cerium-modified Cu-SSZ-13 catalysts were prepared by an aqueous ion-exchange method, and Ce and Cu were incorporated through different ion-exchange sequences. The results of NH₃-SCR activity evaluations displayed that Cu₁(CeCu)₂ catalyst presented excellent catalytic activity, and over 90% NO_x conversion was obtained across the temperature range of 200–500 °C. The characterization results showed that the ion-exchange sequence of Cu and Ce species influenced the crystallinity of the zeolites and the coordination of Al. A small amount of Ce could participate in the reduction process and change the location and coordination environment of copper ions. Furthermore, Ce-modified Cu-SSZ-13 catalysts possessed more acidic sites due to their containing replacement of Ce and movement of Cu in the preparation process. The cooperation of strong redox abilities and NH₃ storage capacity led to the increase of active adsorbed species adsorption and resulted in better activity of Cu₁(CeCu)₂.

Keywords: cerium; Cu-SSZ-13; ion-exchange sequences; SCR; drifts



Citation: Wang, Y.; Li, Z.; Ding, Z.; Kang, N.; Fan, R.; Wang, Y.; Zhang, C.; Guo, X.; Wang, R. Effect of Ion-Exchange Sequences on Catalytic Performance of Cerium-Modified Cu-SSZ-13 Catalysts for NH₃-SCR. *Catalysts* **2021**, *11*, 997. <https://doi.org/10.3390/catal11080997>

Academic Editor: Anker Degn Jensen

Received: 17 June 2021

Accepted: 16 August 2021

Published: 19 August 2021

Publisher's Note: MDPI stays neutral with regard to jurisdictional claims in published maps and institutional affiliations.



Copyright: © 2021 by the authors. Licensee MDPI, Basel, Switzerland. This article is an open access article distributed under the terms and conditions of the Creative Commons Attribution (CC BY) license (<https://creativecommons.org/licenses/by/4.0/>).

1. Introduction

With the rapid development of the economy, environmental issues—especially nitrogen oxides (NO_x) emitted from diesel vehicles—are getting growing attention. There is evidence that states that diesel vehicles accounted for about 10% of automobiles producing nearly 90% of NO_x emitted from automobiles in China. To achieve ultra-low exhaust emission levels, China will implement the China VI Standards to control NO_x pollutants emitted from diesel-fueled, heavy-duty vehicles. In exhaust aftertreatment system of diesel vehicles, the selective catalytic reduction of NO_x with NH₃ (NH₃-SCR) has high efficiency and is currently considered as the most preeminent technology for NO_x removal. Among all catalysts, Cu-SSZ-13 with small-pore structure has been proven to be the most promising catalyst in the NH₃-SCR reaction [1–4].

As we know, the complicated and changeable cold-start and low-load conditions of diesel vehicles make it more challenging for Cu-SSZ-13 catalyst in a wide variety of temperatures (200–600 °C). Also, Cu-SSZ-13 catalyst must have excellent hydrothermal stability, because the SCR unit is located in the high-temperature environment, due to the regeneration of the upstream diesel particle filter (DPF) (above 650 °C) [1]. Recently, several rare earth modified Cu-SSZ-13 catalysts have been widely reported resulting from their easy operability, outstanding de-NO_x efficiency, and high improvement on hydrothermal stability. Usui et al. [5] demonstrated that introduction of a small amount of Ce by wet and solid-state ion-exchange routes could improve SCR activities over a broad temperature

range, because it enabled abundant Brønsted acidity sites and stabilized the framework of SSZ-13. The results of Zhao et al. [6] also confirmed that rare earth ions (Ce^{3+} , La^{3+} , Sm^{3+} , Y^{3+} , Yb^{3+}) that modified Al-rich Cu-SSZ-13 catalysts had no significant impact on low-temperature NO conversions in the fresh catalyst but displayed enhancement of low temperature activity after hydrothermal aging when compared with Cu-SSZ-13. Similarly, Wang et al. [7] reported that Ce or Sm could be introduced into Cu-SSZ-13 by ion exchanged preparation procedures, and the counterparts were investigated in detail. They found that the coexistence of Ce or Sm could exhibit higher hydrothermal stability due to its preventing the framework Al from hydrolysis. Nevertheless, only few research works focused on using different ion-exchange sequences of rare earth and copper ions to modify SSZ-13 zeolite and investigating its NH_3 -SCR performance.

In this study, we prepared Ce-modified Cu-SSZ-13 catalysts by an aqueous ion-exchange method and investigated the effect of different ion-exchange sequences of Cu and Ce on the SCR activity and hydrothermal stability of catalysts. XRD, N_2 adsorption-desorption, as well as ^{29}Si and ^{27}Al NMR were carried out to investigate the textural and structural properties of the Ce-modified Cu-SSZ-13 catalysts. Besides, H_2 -TPR and NH_3 -TPD were used to explore the variation of reduction property and surface acidity.

2. Results and Discussion

2.1. Catalytic Performance

Figure 1 depicted the NH_3 -SCR performance of Cu-SSZ-13 and Ce-modified Cu-SSZ-13 catalysts with the temperature change. As shown in Figure 1a, it can be seen that Cu-SSZ-13 displayed high NO_x conversions (>90%) in the temperature range of 200–400 °C. Note that Cu1(CeCu)2, (CeCu)12 and (CeCu)1Cu2 displayed an enhancement in activity compared with Cu-SSZ-13 at low and high temperatures. In the case of the (CeCu)1Cu2 sample, it showed the highest catalytic performance at 200 °C and nearly 100% NO_x conversion was obtained at this temperature. As compared with Cu-SSZ-13, however, the NO_x conversion of (CeCu)1Cu2 decreased from 71 to 64% at 550 °C and 59 to 52% at 600 °C. For (CeCu)12 and Cu1(CeCu)2, the low-temperature SCR activity (200 °C) and high-temperature activity (>400 °C) were enhanced significantly compared to the NO_x conversions obtained with the Cu-SSZ-13 catalyst. Figure 1b revealed the SCR activity of these four catalysts after hydrothermal aging with 10% H_2O at 850 °C for 10 h under the GHSV of 60,000 h^{-1} . It can be seen that the NO_x conversion of all catalysts decreased to different degrees, but the activity of Cu1(CeCu)2 and (CeCu)1Cu2 was obviously higher than that of Cu-SSZ-13 at high temperature (450–600 °C). Therefore, it was clear that introduction of Ce ions in Cu-SSZ-13 had significant impact on the activity, and Cu1(CeCu)2 was selected as the optimum catalyst due to its excellent NH_3 -SCR performance, and over 90% NO_x conversion of fresh catalyst was obtained across the temperature range of 200–500 °C.

2.2. Textural Properties

The XRD patterns of Cu-SSZ-13 and Ce-modified Cu-SSZ-13 catalysts were shown in Figure 2. It could be seen that all catalysts exhibited a typical chabazite (CHA) crystal structure with characteristic 2θ degrees at 9.6°, 13.0°, 16.1°, 18.1°, 20.7°, 25.2°, 26.3° and 31.0° (PDF data file 52-0784) [8,9]. No noticeable diffraction peaks assigned to Cu species and Ce species were observed indicating that those should be present in the form of isolated ions or highly dispersed on the zeolite crystals [10–12]. There was no obvious difference in diffraction peak position between the catalysts, suggesting the introduced Ce species did not change the CHA structure. The peak intensity had been reported to correlate with the crystallinity of the zeolites [13,14]. As the pattern shown, the intensity of the characteristic peaks of Cu-SSZ-13 and Cu1(CeCu)2 at 9.6° was much higher than that of (CeCu)12 and (CeCu)1Cu2 samples, an effect that might be related to the ion-exchange sequence of the cerium species. As reported by Usui [5], the cerium species in the Cu-SSZ-13 should be present in the form of isolated ions as long as the cerium loading was less than 3 wt.%,

and over 3 wt.% cerium species located at extra ion-exchange sites should not affect the crystallographic features of the zeolite catalyst. This was associated with our observation (Figure 2 and Table 1) and also illustrated that Ce cations in Cu1(CeCu)2, (CeCu)12, and (CeCu)1Cu2 were located at the ion-exchange sites in double six-ring (D6R) or CHA cage.

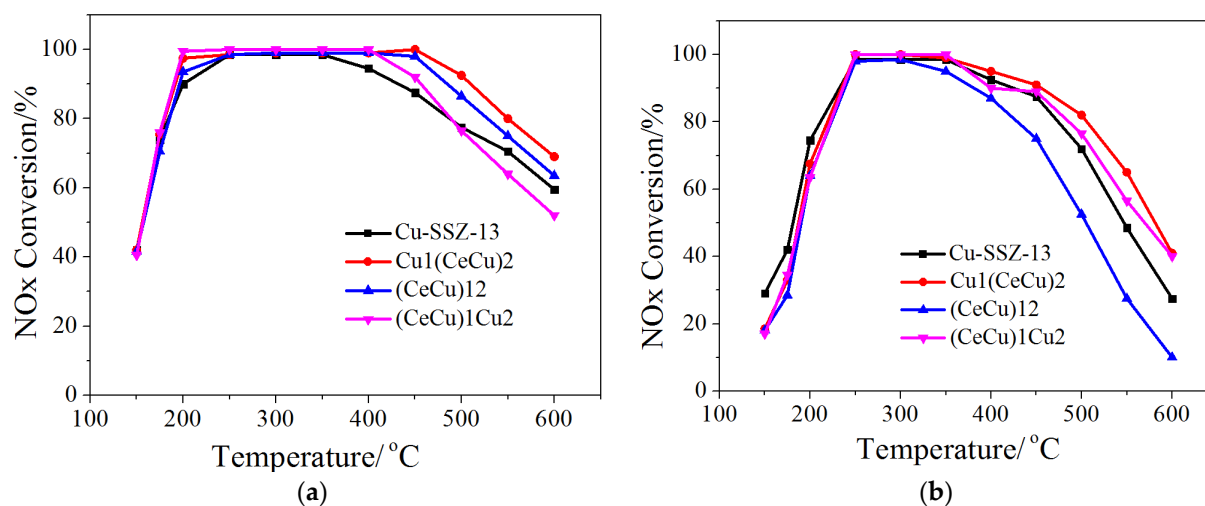


Figure 1. NH₃-SCR performance of fresh (a) and aged (b) Cu-SSZ-13 and Ce-modified Cu-SSZ-13 catalysts.

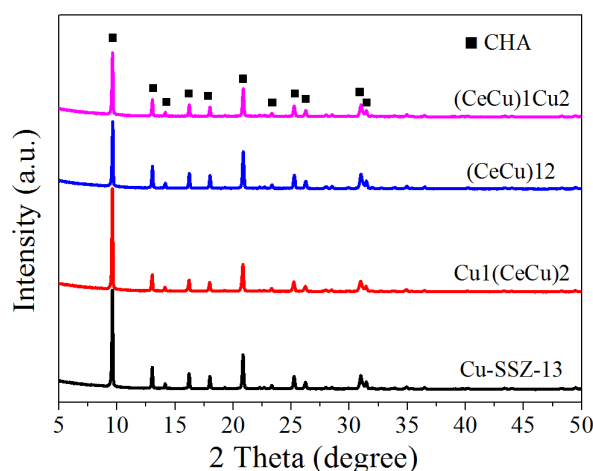


Figure 2. XRD profiles of Cu-SSZ-13 and Ce-modified Cu-SSZ-13 catalysts.

Table 1. Elemental compositions and textural properties over Cu-SSZ-13 and Ce-modified Cu-SSZ-13 catalysts.

Samples	CuO (%) ^a	CeO ₂ (ppm) ^a	Langmuir Surface Area (m ² /g)	V _T (mL/g) ^b
Cu-SSZ-13	1.90	-	793.7	0.2789
Cu1(CeCu)2	1.83	120	763.3	0.2695
(CeCu)12	2.04	130	768.6	0.2730
(CeCu)1Cu2	1.84	60	803.1	0.2779

^a Calculated by ICP. ^b V_T is the t-Plot micropore volume.

Figure 3 presented N₂ adsorption-desorption isotherms and pore width distribution curves over Cu-SSZ-13 and Ce-modified Cu-SSZ-13 catalysts. All samples showed typical type I isotherms according to the BDDT classification, which was consistent with the microporous materials [15,16]. Although the DFT model pore size distribution showed that Cu-SSZ-13, Cu1(CeCu)2, (CeCu)12, and (CeCu)1Cu2 catalysts had only a narrow visible

peak at around 0.73 nm, there was still a little difference in pore size after loading of Ce. The surface area and the t-Plot micropore volume of the prepared catalysts were listed in Table 1. The results showed that all samples had Langmuir surface area over 760 m²/g and total pore volume over 0.26 mL/g.

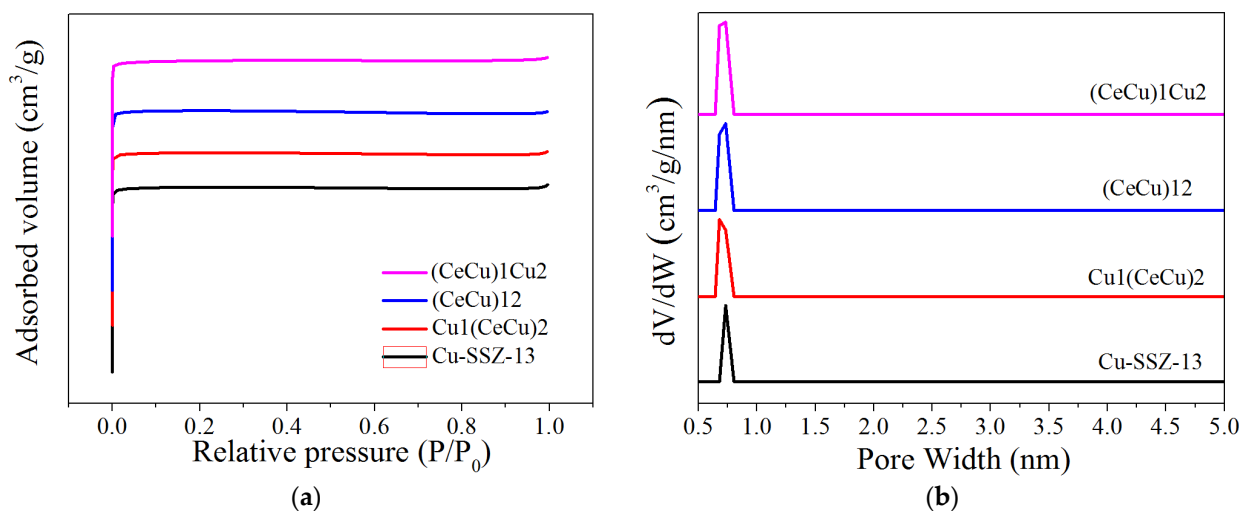


Figure 3. N₂ adsorption-desorption isotherms (a) and pore width distribution curves (b) of the catalysts.

2.3. NMR Measurements

As displayed in Figure 4, solid state NMR measurements were used to monitor the effects of ion-exchange sequence of Cu and Ce species on Al and Si atoms in the framework of SSZ-13. From ²⁷Al NMR spectra (Figure 4a), one resonance feature at a chemical shift of 54 ppm in all these samples was corresponded to tetrahedral Al in the zeolite framework. Meanwhile, a small amount of extra-framework octahedral Al atoms near 5 ppm was observed in the curves of all the catalysts. Apparently, the intensity of the panels over Cu1(CeCu)2, (CeCu)12, and (CeCu)1Cu2 catalysts decreased significantly compared to Cu-SSZ-13, signifying that the introduction of Ce had a great effect on the coordination of Al in molecular sieve. It should be noted that there was a slightly more distorted over Cu-SSZ-13 considering its broader signal because the degree of distortion of the tetrahedral Al was in accordance with the signal width [17,18]. Apparently, the introduction of Ce led the zeolite body to relax and decreased this type of distortion since the signal had narrowed down instead of broadening. However, it was clearly shown that slight skeleton dealumination took place on Ce-modified Cu-SSZ-13 catalysts during the calcination process because of the weak signal intensities. This finding was not consistent with the result of XRD. In the ²⁹Si NMR spectra (Figure 4b), the dominant peak at around 115 ppm was assigned to the presence of tetrahedral Si species (Si(OSi)₄) in the framework, and another weaker feature at 109 ppm was attributed to tetrahedral Si with three Si and one Al neighbor (Si-(OSi)₃-(OAl)) [17–19]. As we know, dealumination would cause the intensity of the 109 ppm signal to decrease [18]. However, it was worth pointing out that intensities for both signals decreased or increased at the same time after the introduction of Ce. Thus, this phenomenon was not a strong indication of the existence of dealumination.

2.4. H₂-TPR Measurements

The H₂-TPR profiles over the Cu-SSZ-13 and Ce-modified Cu-SSZ-13 catalysts were presented in Figure 5. Obviously, all the catalysts exhibited different reduction behaviors, indicating the presence of different Cu and Ce species in the catalysts. For Cu-SSZ-13, the original TPR curve from 170 to 670 °C could be accurately divided into four peaks after peak fitting process on the basis of the Gaussian deconvolution, and each peak corresponded with the reduction of one kind of Cu species. According to literature [20], the peak over

Cu-SSZ-13 appearing at 256 °C was assigned to the reduction of isolated Cu^{2+} ions in the CHA cage. The peak around 368 °C, which was the strongest one in intensity among these H_2 peaks, represented the reduction of Cu^{2+} ions on the D6R. This was consistent with the earlier report that the ion-exchange sites on the D6R were first saturated by Cu^{2+} ions and then coordinated to the CHA cage, and the former required a higher temperature compared to that on other sites because of its highly stable nature in the CHA-type zeolite structure [21]. The high-temperature peak around 406 °C could be attributed to the reduction of Cu^+ to Cu^0 . In addition, the peak located at about 539 °C corresponded to the reduction of highly stable Cu^+ ions to Cu^0 [20,21]. We observed, however, that Ce/Cu-SSZ-13 catalysts exhibited different reducibility properties that depended on the ion-exchange sequence of Cu and Ce species. It was noted that almost all the reduction temperatures of (CeCu)12 and (CeCu)1Cu2 samples shifted to much lower values with respect to Cu-SSZ-13, while a slight difference in the peak temperature between the Cu1(CeCu)2 and Cu-SSZ-13 samples was in fact observed. From this result, we could first conclude that the stability of the zeolite structure of Cu-SSZ-13 and Cu1(CeCu)2 was better than that of (CeCu)12 and (CeCu)1Cu2. Remarkably, with the introduction of Ce to the Cu-SSZ-13 catalysts, a clear increase in the amount of reduction of metal ion on D6R and CHA cage was observed. Also, there was quite a significant increase when computing the total H_2 consumption (shown in Table 2), indicating that the location and coordination environment of copper ions might change, and cerium ions also participated in the reduction process. Besides, comparing the peak concentrations of the reduction of metal ion species could give information about the reducibility of the four samples (Table 2). We further investigated that the ion-exchange sequence of Cu and Ce species influenced the coordination between Cu and Al atoms of the zeolite framework. In particular, the fraction of first peak attributed to $[\text{Cu}(\text{OH})]^+$ in CHA cage in (CeCu)1Cu2 (10.5%) was significantly lower than that of Cu-SSZ-13 (21.8%). On the other hand, as proposed by Usui and coworkers [5], the introduction of Ce in Cu-SSZ-13 should be located in the CHA cage because of the relatively large ionic radius of Ce (1.1 Å). Therefore, it was reasonable to assume that a portion of Ce cations was introduced into CHA cages and replaced the unstable Cu^{2+} ions upon the ion exchange of SSZ-13 in cerium nitrate solutions. On the contrary, we noticed that Ce-modified samples contained higher fractions of more stable Cu^{2+} in D6R, the reduction peak of that, however, was shifted to a lower temperature in (CeCu)12 (347 °C) and (CeCu)1Cu2 (327 °C) compared to ~360 °C for Cu-SSZ-13. Consequently, the ion-exchange sequence of Cu and Ce species influenced the reduction of the catalysts, and the improvement of redox properties over Ce-modified Cu-SSZ-13 samples would be beneficial for the low temperature catalytic reactivity [22]. This was in agreement with the results of the NH_3 -SCR performance.

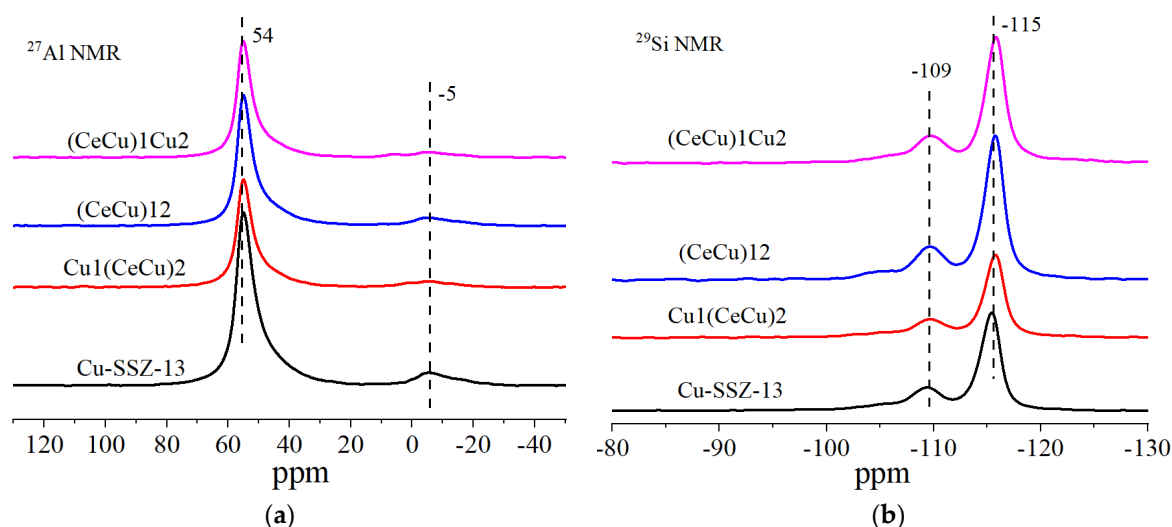


Figure 4. Solid state ^{27}Al (a) and ^{29}Si (b) MAS NMR spectra of Cu-SSZ-13 and Ce-modified Cu-SSZ-13 catalysts.

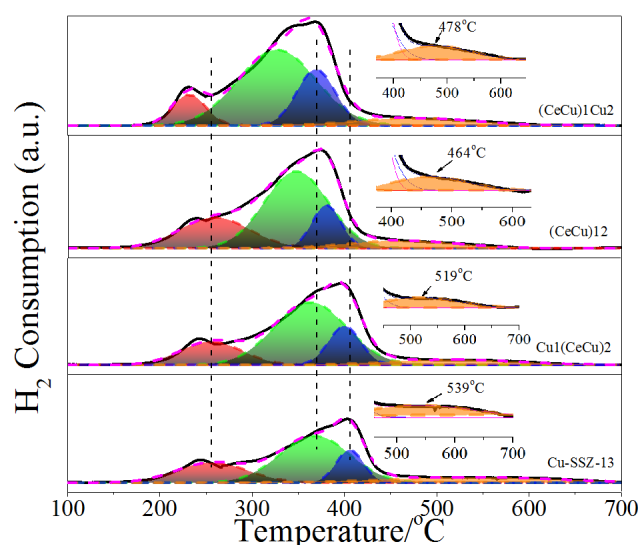


Figure 5. H₂-TPR profiles of Cu-SSZ-13 and Ce-modified Cu-SSZ-13 catalysts.

Table 2. Quantitative analysis of the TPR and TPD profiles of Cu-SSZ-13 and Ce-modified Cu-SSZ-13 catalysts.

Samples	H ₂ Total Consumption (cm ³ /g)	Acidity (cm ³ /g)	Peak Concentration from H ₂ -TPR (%) ^a		X ^b /Cu-SSZ-13 from NH ₃ -TPD (%)	
			Peak 1	Peak 2	Peak 2	Peak 3
Cu-SSZ-13	44.9	32.7	21.8	49.7	-	-
Cu1(CeCu)2	51.0	35.5	18.2	57.3	5.9	3.1
(CeCu)12	62.8	39.1	23.7	53.9	15.2	2.6
(CeCu)1Cu2	76.1	47.8	10.5	59.3	12.4	1.8

^a Peak 1 was the green peak, and peak 2 was the blue peak in Figure 5. ^b X represented Cu1(CeCu)2, (CeCu)12 or (CeCu)1Cu2; Peak 2 and peak 3 were the blue and magenta peak in Figure 6, respectively.

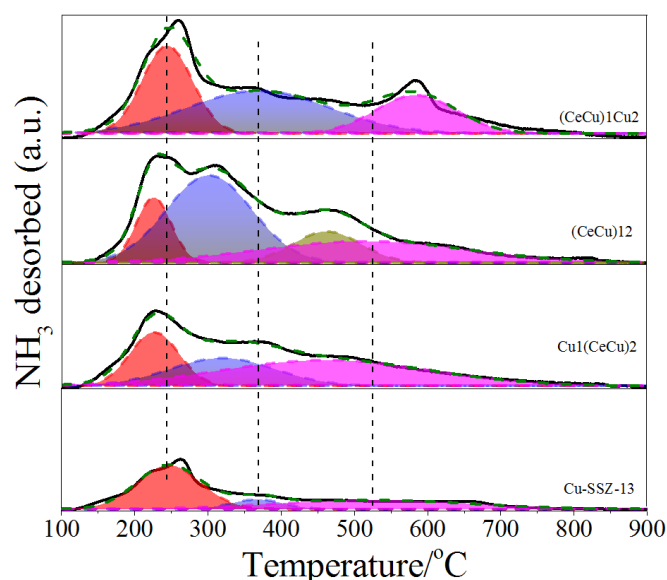


Figure 6. NH₃-TPD profiles of Cu-SSZ-13 and Ce-modified Cu-SSZ-13 catalysts.

2.5. NH₃-TPD Measurements

Through NH₃-TPD measurements, it was possible not only to determine the acidity of the catalyst but also to titrate different acid sites present in zeolite catalysts. The TPD plots of the Cu-SSZ-13 and Ce-modified Cu-SSZ-13 catalysts were presented in Figure 6. The Cu-SSZ-13 was characterized by three NH₃ peaks, and where the peak centered at about

246 °C probably corresponded to NH₃ weakly adsorbed on extra-framework Al Lewis sites or loosely bound ammonia not removed during the purge step, and the NH₃ adsorption peak at around 367 °C represented acid sites in D6R, while the high-temperature (528 °C) peak could be related majorly to NH₃ desorbed from acid sites in CHA cages [7,21,23]. When the catalysts were promoted with Ce ions, the effect of co-cations on the acidity of Cu-SSZ-13 was noteworthy, as an increase in the NH₃ desorption amounts of all the Ce-modified samples was appreciable over the whole desorption temperature range. These results suggested that some new sites were created by Ce species. However, the effect of Ce on the overall NH₃ storage capacity was quite different for the Cu-SSZ-13 with varied ion-exchange sequence of Cu and Ce species. For instance, Cu1(CeCu)2/Cu-SSZ-13 equaled 5.9 for the intermediate peak and 3.1 for the high temperature peak, while the ratios were 15.2, 2.6 and 12.4, 1.8 for (CeCu)12/Cu-SSZ-13 and (CeCu)1Cu2/Cu-SSZ-13 respectively, which was clearly seen in Table 2. Obviously, there was a much larger growth trend of acid sites in CHA cage over Cu1(CeCu)2 catalyst, while the (CeCu)12 and (CeCu)1Cu2 samples maintained higher NH₃ storage capacity in D6R. These different contributions to the NH₃ storage could explain why Ce-modified Cu-SSZ-13 catalysts had different SCR performance when ion-exchange sequence of Cu and Ce species varied. Notice that (CeCu)12 also showed a weak desorption peak at around 463 °C, which might be attributed to the medium-strength acid sites. According to the early report by Wang et al. [7], the ion exchange of Ce could replace a small fraction of unstable [Cu(OH)]⁺ ions in CHA cages. Meanwhile, as reported by Gao et al. [24], the [Cu(OH)]⁺ could convert to “naked” Cu²⁺ ions and move to the sites in windows of 6MR during the dehydration procedure. Taken together with TPR results above, it was reasonable to assume that the extra desorption peak of (CeCu)12 mainly resulted from the movement of [Cu(OH)]⁺ ions. As already shown in literature by Paolucci et al. [25], [Cu(OH)]⁺ and Cu²⁺ differed in their NH₃ coordination behavior: [Cu(OH)]⁺ could be able to coordinate and store 3 NH₃, while Cu²⁺ could store up to 4 NH₃. It was understandable that the sample containing replacement of Ce and movement of Cu in the preparation process could likely form more acidic sites and thus improve the storage capacity of ammonia.

3. Materials and Methods

3.1. Catalyst Preparation

The parent H-SSZ-13 with the mole ratio of SiO₂/Al₂O₃ = 22 was directly provided by Zeolite Company. The initial H-SSZ-13 powder was ion exchanged twice in 0.05 M Cu(CH₃COO)₂ solution at ambient temperature for 6 h, and the ratio of solid to solution was 1:40. After that, the powder was filtered, washed, and calcined at 550 °C for 6 h. Finally, Cu-SSZ-13 catalyst was obtained.

At the same time, the Ce-modified Cu-SSZ-13 catalysts were prepared using the same ion-exchange procedure, and the influence of Ce in the catalyst was controlled by the different exchange sequences with Cu. For the Cu1(CeCu)2 sample, the initial H-SSZ-13 powder was firstly ion exchanged in 0.05 M Cu(CH₃COO)₂ solution at ambient temperature for 6 h. After filtered, washed, and calcined, the powder was added into 0.05 M Cu(CH₃COO)₂ and 0.00625 M Ce(NO₃)₃·6H₂O solution with vigorous stirring for 6 h. Then the powder was filtered, washed, and calcined at 550 °C for 6 h. The (CeCu)12 was produced using ion exchange (twice) of H-SSZ-13 with an aqueous solution of 0.05 M Cu(CH₃COO)₂ and 0.00625 M Ce(NO₃)₃·6H₂O solution at 25 °C for 6 h. Then, the zeolite slurries were filtered, washed with deionized water and calcined at 550 °C for 6 h. For the (CeCu)1Cu2 sample, H-SSZ-13 was exchanged with 0.05 M Cu(CH₃COO)₂ and Ce(NO₃)₃·6H₂O solution firstly and then 0.05 M Cu(CH₃COO)₂ solution at 25 °C for 6 h. After that, the powder was filtered, washed, and calcined at 550 °C for 6 h.

3.2. Catalyst Characterization

XRD was conducted on a Bruker D8 advance (Bruker, Karlsruhe, Baden-Württemberg, Germany); the diffraction angle ranged from 5 to 90 ° using Cu K α radiation at 40 mA

and 40 kV. N₂ adsorption and desorption was conducted on a Micromeritics ASAP 2020 physical adsorption instrument (Micromeritics, Norcross, GA, USA). ²⁹Si and ²⁷Al NMR spectra were carried out on Agilent 600M (Agilent, Palo Alto, CA, USA) utilizing a 4 mm MAS probe. H₂-TPR and NH₃-TPD were performed on an AutoChemII2920 chemisorption analyzer (Micromeritics, Norcross, GA, USA), and the catalyst sample was pretreated under N₂ at 300 °C for 1 h and then cooled down to 50 °C. After that, the catalyst was heated to the required temperature at 10 °C/min in a 5% H₂/Ar or 6000 ppm NH₃/Ar at a flow rate of 50 mL/min.

3.3. Activity Evaluation

De-NO_x tests of catalysts were conducted on a fixed-bed quartz reactor. The gas composition was composed of 200 ppm NH₃, 200 ppm NO, 5% H₂O, 10% O₂, 50 ppm C₃H₆, 4.5% CO₂, 200 ppm CO, and balance N₂. The total gas flow rate was 300 mL·min⁻¹ and the gas hourly space velocity was 250,000 h⁻¹. The concentration of NO_x was monitored by an online flue gas analyzer. The NO_x conversion was calculated as NO_x conversion = $\frac{[\text{NO}_x]_{\text{inlet}} - [\text{NO}_x]_{\text{outlet}}}{[\text{NO}_x]_{\text{inlet}}} \times 100\%$, where NO_x = NO + NO₂ [8].

4. Conclusions

Comparing the Cu-SSZ-13 and Ce-modified Cu-SSZ-13 catalysts synthesized via aqueous ion-exchange, and effects of Ce and Cu ion-exchange sequences on NO_x conversion in NH₃-SCR reaction and the related physical and chemical properties were explored and analyzed in detail. The XRD as well as ²⁷Al and ²⁹Si NMR results indicated that the ion-exchange sequence of Cu and Ce species influenced the crystallinity of the zeolites and the coordination of Al. H₂-TPR demonstrated that the location and coordination environment of copper ions might change after introduction of a small amount Ce, and Ce ions also participated in the reduction process. Moreover, the improvement of redox properties over Ce-modified Cu-SSZ-13 samples would be beneficial for the low temperature catalytic reactivity. NH₃-TPD analysis confirmed that Ce-modified Cu-SSZ-13 catalysts with varied ion-exchange sequence of Cu and Ce species had different NH₃ storage performance, and the sample containing replacement of Ce and movement of Cu in the preparation process could likely form more acidic sites and thus improve the storage capacity of ammonia. The Cu1(CeCu)2 catalyst exchanged Cu firstly and then Ce and Cu at the same time, demonstrating excellent catalytic activity, and over 90% NO_x conversion of fresh catalyst was obtained across the temperature range of 200–500 °C. Therefore, the cooperation of strong redox abilities and NH₃ storage capacity led to the increase of active adsorbed species adsorption and resulted in the better activity of Cu1(CeCu)2.

Author Contributions: Conceptualization, Y.W. (Yan Wang); Investigation, Y.W. (Yan Wang), Z.D., N.K., R.F., C.Z., Y.W. (Yu Wang), R.W. and X.G.; Data Curation, Y.W. (Yan Wang); Writing—Review & Editing, Y.W. (Yan Wang); Supervision, Z.L.; Project Administration, Z.L. All authors have read and agreed to the published version of the manuscript.

Funding: This research received no external funding.

Data Availability Statement: Data is contained within the article.

Conflicts of Interest: The authors declare no conflict of interest.

References

1. Shan, Y.L.; Du, J.P.; Zhang, Y.; Shan, W.P.; Shi, X.Y.; Yu, Y.B.; Zhang, R.D.; Meng, X.J.; Xiao, F.S.; He, H. Selective catalytic reduction of NO_x with NH₃: Opportunities and challenges of Cu-based small-pore zeolites. *Natl. Sci. Rev.* **2021**, *8*, 1–10.
2. Clark, A.H.; Nuguid, R.J.G.; Steiger, P.; Marberger, A.; Petrov, A.W.; Ferri, D.; Nachttegaal, M.; Kröcher, O. Selective catalytic reduction of NO with NH₃ on Cu-SSZ-13: Deciphering the low and high-temperature rate-limiting steps by transient XAS experiments. *ChemCatChem* **2020**, *12*, 1429–1435. [[CrossRef](#)]
3. Chen, M.Y.; Sun, Q.M.; Yang, X.G.; Yu, J.H. A dual-template method for the synthesis of bimetallic CuNi/SSZ-13 zeolite catalysts for NH₃-SCR reaction. *Inorg. Chem. Commun.* **2019**, *105*, 203–207. [[CrossRef](#)]

4. Bendrich, M.; Scheuer, A.; Hayes, R.E.; Votsmeier, M. Increased SCR performance of Cu-CHA due to ammonium nitrate buffer: Experiments with oscillating NO/NO₂ ratios and application to real driving cycles. *Appl. Catal. B Environ.* **2020**, *270*, 118763–118771. [[CrossRef](#)]
5. Usui, T.; Liu, Z.D.; Ibe, S.; Zhu, J.; Anand, C.; Igarashi, H.; Onaya, N.; Sasaki, Y.; Shiramata, Y.; Kusamoto, T.; et al. Improve the hydrothermal stability of Cu-SSZ-13 zeolite catalyst by loading a small amount of Ce. *ACS Catal.* **2018**, *8*, 9165–9173. [[CrossRef](#)]
6. Zhao, Z.C.; Yu, R.; Shi, C.A.; Gies, H.; Xiao, F.S.; Vos, D.D.; Yokoi, T.; Bao, X.H.; Kolb, U.; McGuire, R.; et al. Rare-earth ion exchanged Cu-SSZ-13 zeolite from organotemplate-free synthesis with enhanced hydrothermal stability in NH₃-SCR of NO_x. *Catal. Sci. Technol.* **2019**, *9*, 241–251. [[CrossRef](#)]
7. Wang, Y.J.; Shi, X.Y.; Shan, Y.L.; Du, J.P.; Liu, K.; He, H. Hydrothermal stability enhancement of Al-Rich Cu-SSZ-13 for NH₃ selective catalytic reduction reaction by ion eExchange with cerium and samarium. *Ind. Eng. Chem. Res.* **2020**, *59*, 6416–6423. [[CrossRef](#)]
8. Fan, J.; Ning, P.; Wang, Y.C.; Song, Z.X.; Liu, X.; Wang, H.M.; Wang, J.; Wang, L.Y.; Zhang, Q.L. Significant promoting effect of Ce or La on the hydrothermal stability of Cu-SAPO-34 catalyst for NH₃-SCR reaction. *Chem. Eng. J.* **2019**, *369*, 908–919. [[CrossRef](#)]
9. Wang, Y.; Li, Z.Q.; Fan, R.R.; Guo, X.; Zhang, C.; Wang, Y.; Ding, Z.Y.; Wang, R.; Liu, W. Deactivation and regeneration for the SO₂-poisoning of a Cu-SSZ-13 catalyst in the NH₃-SCR reaction. *Catalysts* **2019**, *9*, 797. [[CrossRef](#)]
10. Liang, J.; Mi, Y.; Song, G.; Peng, H.G.; Li, Y.L.; Yan, R.; Liu, W.M.; Wang, Z.; Wu, P.; Liu, F.D. Environmental benign synthesis of Nano-SSZ-13 via FAU transcrystallization: Enhanced NH₃-SCR performance on Cu-SSZ-13 with nanosize effect. *J. Hazard. Mater.* **2020**, *398*, 122986–122998. [[CrossRef](#)]
11. He, D.D.; Wang, Z.H.; Deng, D.; Deng, S.J.; He, H.; Liu, L.C. Synthesis of Cu-SSZ-13 catalyst by using different silica sources for NO-SCR by NH₃. *Mol. Catal.* **2020**, *484*, 110738–110747. [[CrossRef](#)]
12. Wang, Y.; Nishitoba, T.; Wang, Y.N.; Meng, X.J.; Xiao, F.S.; Zhang, W.P.; Marler, B.; Gies, H.; Vos, D.D.; Kolb, U.; et al. Cu-exchanged CHA-Type zeolite from organic template-free synthesis: An effective catalyst for NH₃-SCR. *Ind. Eng. Chem. Res.* **2020**, *59*, 7375–7382. [[CrossRef](#)]
13. Su, W.K.; Li, Z.G.; Peng, Y.; Li, J.H. Correlation of the changes in the framework and active Cu sites for typical Cu/CHA zeolites (SSZ-13 and SAPO-34) during hydrothermal aging. *Phys. Chem. Chem. Phys.* **2015**, *17*, 29142–29149. [[CrossRef](#)] [[PubMed](#)]
14. Ma, L.; Cheng, Y.S.; Cavataio, G.; McCabe, R.W.; Fu, L.X.; Li, J.H. Characterization of commercial Cu-SSZ-13 and Cu-SAPO-34 catalysts with hydrothermal treatment for NH₃-SCR of NO_x in diesel exhaust. *Chem. Eng. J.* **2013**, *225*, 323–330. [[CrossRef](#)]
15. Jiang, H.; Guan, B.; Lin, H.; Huang, Z. Cu/SSZ-13 zeolites prepared by in situ hydrothermal synthesis method as NH₃-SCR catalysts: Influence of the Si/Al ratio on the activity and hydrothermal properties. *Fuel* **2019**, *255*, 15587–115604. [[CrossRef](#)]
16. Cui, Y.R.; Wang, Y.L.; Walter, E.D.; Szanyi, J.; Wang, Y.; Gao, F. Influences of Na⁺ co-cation on the structure and performance of Cu/SSZ-13 selective catalytic reduction catalysts. *Catal. Today* **2020**, *339*, 233–240. [[CrossRef](#)]
17. Wang, J.C.; Peng, Z.L.; Qiao, H.; Yu, H.F.; Hu, Y.F.; Chang, L.P.; Bao, W.R. Cerium-stabilized Cu-SSZ-13 catalyst for the catalytic removal of NO_x by NH₃. *Ind. Eng. Chem. Res.* **2016**, *55*, 1174–1182. [[CrossRef](#)]
18. Luo, J.Y.; Gao, F.; Kamasamudram, K.; Currier, N.; Peden, C.H.F.; Yezerets, A. New insights into Cu/SSZ-13 SCR catalyst acidity. Part I: Nature of acidic sites probed by NH₃ titration. *J. Catal.* **2017**, *348*, 291–299. [[CrossRef](#)]
19. Zhang, T.; Qiu, F.; Li, J.H. Design and synthesis of core-shell structured meso-Cu-SSZ-13@mesoporous aluminosilicate catalyst for SCR of NO_x with NH₃: Enhancement of activity, hydrothermal stability and propene poisoning resistance. *Appl. Catal. B Environ.* **2016**, *195*, 48–58. [[CrossRef](#)]
20. Kim, Y.J.; Lee, J.K.; Min, K.M.; Hong, S.B.; Nam, I.S.; Cho, B.K. Hydrothermal stability of CuSSZ13 for reducing NO_x by NH₃. *J. Catal.* **2014**, *311*, 447–457. [[CrossRef](#)]
21. Villamaina, R.; Liu, S.J.; Nova, I.; Tronconi, E.; Ruggeri, M.P.; Collier, J.; York, A.; Thompsett, D. Speciation of Cu cations in Cu-CHA catalysts for NH₃-SCR: Effects of SiO₂/AlO₃ ratio and Cu-loading investigated by transient response methods. *ACS Catal.* **2019**, *9*, 8916–8927. [[CrossRef](#)]
22. Shan, W.; Geng, Y.; Chen, X.; Huang, N.; Liu, F.; Yang, S. A highly efficient CeWO_x catalyst for the selective catalytic reduction of NO_x with NH₃. *Catal. Sci. Technol.* **2016**, *6*, 1195–1200. [[CrossRef](#)]
23. Leistner, K.; Xie, K.P.; Kumar, A.; Kamasamudram, K.; Olsson, L. Ammonia Desorption Peaks Can Be Assigned to Different Copper Sites in Cu/SSZ-13. *Catal. Lett.* **2017**, *147*, 1882–1890. [[CrossRef](#)]
24. Gao, F.; Washton, N.M.; Wang, Y.; Kollar, M.; Szanyi, J.; Peden, C.H.F. Effects of Si/Al ratio on Cu/SSZ-13 NH₃-SCR catalysts: Implications for the active Cu species and the roles of Brønsted acidity. *J. Catal.* **2015**, *331*, 25–38. [[CrossRef](#)]
25. Paolucci, C.; Parekh, A.A.; Khurana, I.; Di Iorio, J.R.; Li, H.; Albarracin Caballero, J.D.; Shih, A.J.; Anggara, T.; Delgass, W.N.; Miller, J.T.; et al. Catalysis in a cage: Condition-dependent speciation and dynamics of exchanged Cu cations in SSZ-13 zeolites. *J. Am. Chem. Soc.* **2016**, *138*, 6028–6048. [[CrossRef](#)] [[PubMed](#)]